INFECTION AND IMMUNITY, Oct. 2004, p. 5582–5596 Vol. 72, No. 10
0019-9567/04/$08.00+0 DOI: 10.1128/IAI.72.10.5582–5596.2004

Microarray Analysis of Pneumococcal Gene Expression during Invasive Disease

Carlos J. Orihuela,[1] Jana N. Radin,[1,2] Jack E. Sublett,[1] Geli Gao,[1] Deepak Kaushal,[3] and Elaine I. Tuomanen[1,2]*

Department of Infectious Diseases[1] and Hartwell Center for Bioinformatics and Biotechnology,[3] St. Jude Children's Research Hospital, and Department of Molecular Sciences, University of Tennessee Health Science Center,[2] Memphis, Tennessee

Received 23 March 2004/Returned for modification 19 May 2004/Accepted 29 June 2004

***Streptococcus pneumoniae* is a leading cause of invasive bacterial disease. This is the first study to examine the expression of *S. pneumoniae* genes in vivo by using whole-genome microarrays available from The Institute for Genomic Research. Total RNA was collected from pneumococci isolated from infected blood, infected cerebrospinal fluid, and bacteria attached to a pharyngeal epithelial cell line in vitro. Microarray analysis of pneumococcal genes expressed in these models identified body site-specific patterns of expression for virulence factors, transporters, transcription factors, translation-associated proteins, metabolism, and genes with unknown function. Contributions to virulence predicted for several unknown genes with enhanced expression in vivo were confirmed by insertion duplication mutagenesis and challenge of mice with the mutants. Finally, we cross-referenced our results with previous studies that used signature-tagged mutagenesis and differential fluorescence induction to identify genes that are potentially required by a broad range of pneumococcal strains for invasive disease.**

Streptococcus pneumoniae is the primary cause of community-acquired pneumonia and a major cause of invasive bacterial disease (28). Each year in the United States, pneumococci are responsible for 100,000 to 135,000 hospitalizations for pneumonia, 50,000 cases of bacteremia, and 3,000 cases of meningitis (18). Worldwide these diseases account for more than a million deaths a year. Currently, a 7-valent polysaccharide-protein conjugate vaccine is effective; however, it protects against only a small subset of the serotypes known to cause invasive disease (9). Invasive disease follows colonization of the nasopharynx and is the result of spread of the bacteria to the lungs and blood. Once in the bloodstream, infection may result in septicemia or meningitis, both of which have high mortality despite accepted antibiotic therapy (28).

Since Pasteur and Sternberg first described the pneumococcus, a number of virulence factors required for invasive disease have been identified. Major virulence determinants such as capsular polysaccharide, pneumolysin, and choline-binding proteins have clearly established roles in pathogenesis (18). More recently, large-scale identification of *S. pneumoniae* virulence determinants has been attempted. Studies, such as signature-tagged mutagenesis (STM), have used transposons and suicide vectors to pepper the chromosome of the bacteria with mutations and identify genes required for virulence (13, 25, 39). STM screens rely on negative selection of mutants through passage in animal models and, to date, STM has been used three times for the pneumococcus, each time in a different strain.

Ideally, characterization of pneumococcal virulence determinants should include analysis of gene expression during invasive disease. Confirmation of their expression in vivo would not only verify the contribution of these genes to pathogenesis but would also elucidate their contribution to discrete forms of disease (e.g., genes expressed during pneumonia versus those in the blood during bacteremia). Unfortunately, analysis of in vivo bacterial gene expression, much less at discrete sites, has been limited by the difficulties of isolating sufficient quantities of pure and intact bacterial RNA from infected host tissues. To circumvent the requirement for RNA, investigators have used differential fluorescence induction (DFI) to identify *S. pneumoniae* promoters that are induced during disease (29). In contrast to STM, DFI relies on the promoter activity of random fragments of DNA cloned upstream of an episomal, promoterless green fluorescent protein. Fluorescence is imparted by the promoter activity of the randomly integrated DNA fragment under the environmental conditions tested (in vivo). Fluorescent bacteria can then be sorted by fluorescence-activated cell sorting analysis, leaving only bacteria containing plasmids with active promoters. Using DFI, Marra et al. identified operons that are enhanced during bacterial growth in a chinchilla model of otitis media, lower respiratory tract infection in a mouse, and growth in an intraperitoneal chamber implant model (29).

Large-scale analysis of gene expression during invasive disease provides not only transcriptional data with regard to certain genes, such as virulence determinants but, after interpretation, also provides information as to the status of the bacteria during infection and the response of the bacteria to the host environment. In vivo gene expression therefore potentially identifies unknown or unappreciated targets for pharmaceutical or vaccine intervention since, presumably, the genes whose transcription is altered during invasive disease are those that are required by the bacteria for survival in the host (14).

* Corresponding author. Mailing address: St. Jude Children's Research Hospital, Mailstop 320, IRC 8057, 332 North Lauderdale Rd., Memphis, TN 38105. Phone: (901) 495-3486. Fax: (901) 495-3099. E-mail: elaine.tuomanen@stjude.org.

We describe here a protocol for the collection of RNA from bacteria within infected blood and cerebrospinal fluid (CSF) in vivo and bacteria adherent to epithelial cells in vitro. Using genome-wide cDNA microarrays available from the Pathogen Functional Genomic Research Center (PFGRC) at The Institute for Genomic Research (TIGR; Rockville, Md.), we have examined pneumococcal gene expression during bacteremia, meningitis, and epithelial cell contact (ECC). Analysis of pneumococcal genes expressed in these models identified global patterns of expression unique to each condition tested. Patterns of expression were identified with regard to virulence factors, transporters, transcription factors, translation-associated proteins, metabolism, and genes with unknown function. These findings were then cross referenced to previous STM and DFI studies. Finally, we examined several candidate virulence genes with unknown function by insertion duplication mutagenesis and challenge of mice.

MATERIALS AND METHODS

Media and growth conditions. *S. pneumoniae* was grown on tryptic soy agar (Difco, Detroit, Mich.) supplemented with 3% defibrinated sheep blood or in defined semisynthetic casein liquid medium (24) supplemented with 0.5% yeast extract (C+Y). Erythromycin (1 μg/ml) and kanamycin (400 μg/ml) (Sigma, St. Louis, Mo.) were added to the growth medium as appropriate. *S. pneumoniae* cultures were inoculated from frozen stock and incubated at 37°C in 5% CO_2. *Escherichia coli* strains were grown in Luria-Bertani medium (Difco) at 37°C in an orbital shaker; erythromycin (1 mg/ml) was added to the *E. coli* cultures to maintain any plasmids.

Bacterial strains and construction of mutants. D39 Xen7 (D39X), a stable bioluminescent isolate of *S. pneumoniae*, serotype 2, strain D39 (2), was created as previously described (11). TIGR4 Xen 35 (T4X) was created by transformation of TIGR4 with genomic DNA from D39X by using CSP-2 (35). Bioluminescent mutants deficient in genes identified as enhanced during invasive disease were created by insertion duplication mutagenesis (37). PCR primers with nested EcoRI and BamHI restriction sites were used to amplify 200- to 500-bp fragments from the N termini of the genes. Amplified PCR fragments were purified and digested with EcoRI and BamHI (New England BioLabs, Beverly, Mass.). Digested fragments were ligated into the vector pJDC9 and transformed into chemically competent XL1-Blue *E. coli* (Stratagene, La Jolla, Calif.). Single transformants containing the insert were identified and plasmid DNA from these clones was used to transform D39X by using CSP-1 or, alternatively, T4X with CSP-2 (7). Chromosomal integration of the vector at the correct locus was verified by PCR analysis and sequencing by using a primer contained within the integrated vector and a primer upstream of the gene of interest.

Isolation of bacterial RNA from infected mouse blood. Female BALB/cJ mice (4 to 5 weeks old; The Jackson Laboratory, Bar Harbor, Maine) were maintained in a biosafety level 2 facility at St. Jude Children's Research Hospital. All experimental procedures were done with mice anesthetized with either inhaled isoflurane (Baxter Healthcare Corp., Deerfield, Ill.) at 2.5% or intraperitoneal MKX (1 ml of ketamine [Fort Dodge Laboratories, Fort Dodge, Iowa] at 100 mg/ml; 5 ml of xylazine [Miles Laboratories, Shawnee Mission, KA] at 100 mg/ml; 21 ml of phosphate-buffered saline [PBS]) at 5 μl/g of body weight. Bacteria in the blood were collected by using a modified version of the protocol described by Ogunniyi et al. (33). Mice were infected intratracheally with 10^5 CFU of D39X and imaged by using a charge-coupled device camera at 48 h postchallenge. Mice with severe sepsis, as determined by bioluminescent imaging (>50,000 relative light units/mouse) (11), were exsanguinated, and the blood was immediately transferred to a tube containing RNAprotect (Qiagen, Valencia, Calif.) at a ratio of 35:1 (vol/vol; RNAprotect/expected total mouse blood collected) and vortexed for 5 s. Bacteria were harvested by centrifugation of the suspension at 825 × *g* for 10 min to remove debris, followed by centrifugation at 15,000 × *g* for 15 min to pellet the bacteria. RNA isolation was performed by using a Qiagen RNeasy minikit (Qiagen) with the following modifications. Bacteria were lysed in the presence of 400 mg of 0.1-mm zirconia-silica beads (BioSpec Products, Inc., Bartlesville, Okla.) by using the Mini-Beadbeater 3110BX (BioSpec Products, Inc.) and then incubated at 70° C for 10 min. Bacterial lysate was spun through a Qiashredder column (Qiagen) to remove the beads, and the remaining solution was subsequently processed according to the manufacturer's protocol with an on-column DNase digestion step. Quantitation of RNA was performed by using a UV spectrophotometer (UV-1601; Shimadzu Corp., Kyoto, Japan) at an optical density at 260 nm (OD_{260}), whereas degradation was assessed by visualization of the RNA on a 1% agarose Tris-borate-EDTA (TBE) gel.

Isolation of bacterial RNA from infected rabbit CSF. Male New Zealand White rabbits (5 kg; Myrtles, Thompson Station, Tenn.) were anesthetized with 35 ml of 25% urethane administered subcutaneously and pentobarbital sodium (15 mg/kg) given intravenously. Anesthetized rabbits were immobilized on a stereotaxic frame and challenged by direct intracisternal injection with 10^8 CFU of T4X by using a 25-gauge spinal needle (27). At 4 h after challenge, CSF was collected and transferred immediately to a sterile tube containing RNAprotect at a ratio of 3:1 (RNAprotect/rabbit CSF). RNA was then collected as described above.

Isolation of bacterial RNA from pneumococci attached to Detroit cells. A T-175 flask of confluent Detroit pharyngeal epithelial cells (38) was activated with tumor necrosis factor alpha (Sigma) at 10 ng/ml for 2 h. Cells were challenged with 25 ml of a 4×10^6-CFU/ml suspension of T4R (12), an unencapsulated derivative of TIGR4, and incubated at 37°C for 3 h to allow for adherence. After the incubation, cells were washed three times with PBS (BioWhittaker, Walkersville, Md.) to remove nonadherent bacteria and covered with 10 ml of RNAprotect. Cells were scraped off the surface of the flask, and the suspension was transferred to a new T-175 flask containing 3-mm glass beads. Cells were sonicated for 5 min by using a tabletop ultrasonic cleaner (FS20; Fisher Scientific, Pittsburgh, Pa.) to lyse the epithelial cells but leave the bacteria intact. The suspension was then centrifuged at 800 × *g* for 5 min to remove cellular debris and then centrifuged at 4,600 × *g* for 10 min to pellet the bacteria. RNA was collected from the bacterial/eukaryotic pellet by using a Qiagen RNeasy minikit. To remove the remaining eukaryotic RNA, bacterial RNA isolated from the bacterial/eukaryotic pellet was then enriched by using MICROBEnrich (Ambion, Austin, Tex.). Quantitation of RNA was performed by using a UV spectrophotometer at OD_{260}, whereas degradation was assessed by visualization of the RNA on a 1% agarose TBE gel. As a control, RNA was collected from bacteria grown in tissue culture medium in parallel and was processed by using MICROBEnrich.

Microarray analysis of bacterial RNA. Microarray experiments were performed by using whole-genome *S. pneumoniae* cDNA microarrays obtained from the PFGRC at TIGR (http://pfgrc.tigr.org.). The *S. pneumoniae* genome microarray consisted of PCR products representing segments of 2,131 open reading frames from *S. pneumoniae* strain TIGR4 (44) and 118 unique open reading frames from strains R6 (17) and G54 (39). Microarray experiments, including RNA quality control, Cy3 and Cy5 dye labeling, hybridization, washing, and scanning, were performed at the Functional Genomics lab, Hartwell Center for Bioinformatics and Biotechnology, St. Jude Children's Research Hospital, by using protocols from the PFGRC (http://pfgrc.tigr.org/protocols.shtml). The hybridization probe was constituted by mixture of differentially labeled cDNA derived from (i) total RNA isolated from *S. pneumoniae* obtained from either infected mouse blood or rabbit CSF or (ii) RNA from bacteria grown in C+Y. Alternatively, probe for ECC analysis was constituted with (i) RNA isolated from bacteria adhered to Detroit cells or (ii) RNA from parallel cultures grown in tissue culture media. RNA samples from both conditions were labeled with monofunctional Cy3 and Cy5 dyes by using an indirect amino-allyl labeling method, combined, and hybridized overnight to the printed slides. Slides were washed and scanned by using an Axon 4000B dual channel scanner (Axon Corp., Union City, Calif.) to generate a multi-TIFF image of each slide. Images were analyzed by using Axon GenePix 4.1 image analysis software, and the resulting text-data files were imported into Spotfire DecisionSite for Functional Genomics (version 7.2; Spotfire, Sommerville, Mass.). A series of filtration algorithms were applied to remove spots that consistently generated bad data (based on the frequency with which a particular spot failed to reach a minimum required signal-to-noise ratio [SNR] and the frequency with which a particular spot was flagged bad by the image analysis software GenePix Pro 4.1). Genes that were flagged ≥66% of the time were removed from analysis. Similarly, spots that failed to meet the SNR criteria 75% of the time (9 of 12 times for blood and ECC microarrays and 6 of 8 for CSF microarrays) were removed from consideration. Intensity-based global normalization was then performed to remove dye-specific bias, and background correction was performed by subtracting the normalized median pixel intensity of the background value from the normalized median pixel intensity of the spot itself. Cy5/Cy3 ratios (fold changes) were then calculated for every spot. Since each gene was spotted four times per glass microarray, only genes whose corresponding spots were not flagged at least 75% of the times were considered.

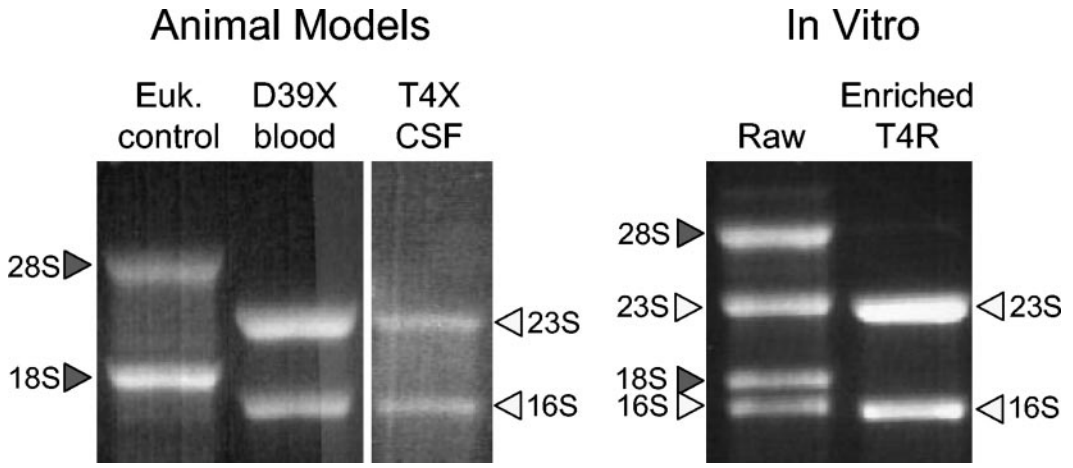

FIG. 1. RNA collected from *S. pneumoniae* in vivo and in vitro. After isolation of pneumococcal RNA from infected blood, CSF, and bacteria adherent to the Detroit pharyngeal epithelial cell line, RNA was visualized on a 1% TBE gel to confirm purity and assess degradation. Bacterial RNA (open arrowheads) and eukaryotic RNA (shaded arrowheads) are indicated. Bacterial RNA isolated from the ECC model was enriched after collection of the initial pellet (raw) to remove contaminating eukaryotic RNA.

Statistical analysis of microarray data. Microarray analysis examining RNA from bacteria adhered to Detroit cells and blood experiments was performed on total RNA isolated from three independent biological replicate experiments. Microarray analysis examining RNA from infected rabbit CSF was performed on total RNA isolated from two independent biological replicate experiments. Accuracy and statistical significance of the gene expression differential over the course of the replicate experiments was calculated by using a Student *t* test-analysis of variance algorithm available in Spotfire DecisionSite (19). Genes with high levels of significance ($P > 0.001$) and a minimum fold change of 2.0 were considered up- or downregulated.

Virulence assessment of mutants. To assess the virulence potential of mutants deficient in genes with altered expression in vivo, mice were challenged intratracheally and monitored for 4 days or challenged intranasally and monitored for 7 days. Exponential cultures (OD_{620} = 0.5) of D39X, T4X, or their derivatives were centrifuged, and the bacteria were washed with and suspended in PBS. Mice were anesthetized with isoflurane and challenged intranasally with 10^7 CFU in 25 μl or intratracheally with 10^5 CFU in 100 μl of PBS. At 2 days postchallenge, all mice were sampled by intranasal lavage, blood collection from the tail vein, and bioluminescent imaging with a Xenogen IVIS camera. Bioluminescent imaging provided a noninvasive method for assessing the bacterial burden in the lungs of all of the mice (data not shown). After imaging, 6 to 10 mice were randomly selected from each cohort and sacrificed, and bacterial titers in lungs were determined. The number of CFU present per gram of homogenized lungs was used to assess bacterial burden in the lungs. Remaining mice (6 to 10 per group) were then observed to determine the percent survival over time. In all instances after challenge, the infectious dose was confirmed by serial dilution and plating of the bacterial suspension on blood agar.

RESULTS AND DISCUSSION

Microarray analysis is a powerful tool for transcriptional analysis of pneumococcal gene expression during invasive disease. Provided RNA is obtainable, microarrays directly measure transcription for each gene on the chromosome at once. To date, however, pneumococcal microarrays have only been used to examine bacteria in vitro, more specifically, to examine the pneumococcal response to a particular environment or to examine isogenic mutants. In the present study, we describe for the first time microarray analysis of in vivo gene expression during bacteremia and meningitis. We also examine gene expression in response to intimate contact of the pneumococcus with epithelial cells in vitro.

Collection of RNA samples from infected blood and CSF. Collection of bacterial RNA from infected tissues has been limited by the inherent difficulties of separating large quantities of host cells and debris away from bacteria in a manner sufficiently timely to prevent degradation of RNA or to prevent novel gene expression in response to conditions presented during the separation process (14, 36). To avoid these problems, we harvested infected mouse blood and rabbit CSF directly into RNAprotect (Qiagen). RNAprotect served to stabilize bacterial RNA, allowed purification of the RNA without degradation (Fig. 1), and lysed contaminating host cells. Preliminary experiments determined that high titers of bacteria ($>10^8$ CFU/ml) in body fluids were required to obtain sufficient RNA (data not shown). Although strain T4X was used for meningitis, preliminary experiments determined its yield in blood was too low (data not shown). Therefore, for bacteremia we used strain D39, which attains titers in blood of 10^9 CFU/ml by 48 h after challenge (35). Bioluminescence of T4X and D39X permitted visualization of the bacteria in living mice and allowed us to identify animals with sufficiently high bacterial titers for RNA isolation. Bioluminescent imaging was necessary, since only half of the mice infected intratracheally had sufficient bacteria in the bloodstream 48 h postchallenge. The remaining mice eventually progressed to similar levels of bacteremia ($\sim 10^9$ CFU/ml of blood within 12 to 24 h); however, this occurred in a manner too staggered for satisfactory bacteria collection. Exsanguination of the mice collected at 48 h yielded ~0.75 ml of blood from each infected animal, which in turn allowed collection of ~25 μg of pure bacterial RNA from the pooled blood of three to four mice.

Sufficient bacteria could be harvested from the CSF of infected rabbits only upon challenge with 10^8 CFU of T4X (35); strain D39X did not grow to a sufficiently high titer. T4X is a derivative of TIGR4 (44), the fully sequenced clinical isolate obtained from a child with meningitis. At 4 h after intracisternal challenge, ~1.0 ml of infected CSF was collected and yielded ~5 μg of pure bacterial RNA from each rabbit (Fig. 1).

Collection of RNA samples from pneumococci attached to epithelial cells. To examine bacterial gene expression in response to ECC, we infected confluent monolayers of Detroit cells (38), a pharyngeal epithelial cell line, with pneumococcus T4R. T4R is an unencapsulated derivative of T4 (12). As a control, RNA was collected from bacteria grown in the same tissue culture media without cells. These analyses therefore reflect only changes in gene expression that are a result of host cell exposure. Stimuli resulting in alterations in gene expression should therefore be limited to (i) intimate contact with the host cells, (ii) soluble factors released by the host cell during normal processes, and (iii) soluble factors released by the host cell in response to the bacterial infection. Collection of RNA from bacteria attached to Detroit cells resulted in the collection of ~25 μg of mixed eukaryotic and prokaryotic RNA from the bacteria and host cell pellet. Using MICROBencrich, we were able to purify the prokaryotic RNA (Fig. 1), with a final yield of ~10 μg per T-175 flask.

Microarray analysis of gene expression relies on the comparison of two RNA species. Levels of expression reported in the test condition are reported in relation to levels of transcription observed in the control condition. A direct comparison of test versus control can be set up in vitro with tissue culture (medium to medium plus Detroit cells). With regard to in vivo gene expression, an appropriate in vitro control condition does not exist. However, reference to the same arbitrary control media (blood versus C+Y or CSF versus C+Y) allows for indirect comparisons between the different test conditions (blood versus CSF). As a baseline, >99% of genes showed similar expression levels in D39 and T4 grown in C+Y (data not shown).

Microarray analysis of bacterial physiology in different body sites. Filtration algorithms and SNR analysis of the microarrays by GenePix 4.1 removed genes whose corresponding spots on the microarray were not valid ≥75% of the time. As such, the results reported in the present study correspond to 69% of the genome during growth in the bloodstream, 53% of the genome during meningitis, and 68% of the genome after ECC. A list of the genes that did not meet the above criteria and therefore were not analyzed for alternate gene expression in vivo can be found at http://www.stjuderesearch.org/vivogene. Stringent requirements imposed by the filtration algorithms ensured that any alterations in gene expression that are reported here are rigorously supported by the data collected from the microarrays.

For genes that met the established criteria for transcription analysis, it was determined that the majority (92% in the blood, 85% in CSF, and 90% after ECC) were expressed in a fashion similar to growth in C+Y. Table 1 lists the genes with altered transcription sorted based on their putative cellular role and their location on the bacterial chromosome. Inclusion criteria were a >2-fold change in levels of expression and a *P* value of <0.01. Of the genes with altered expression in vivo, 55% had enhanced expression in blood, while 81% were enhanced during ECC. In contrast, only 35% were enhanced during growth in CSF. Overall, the patterns of gene expression were determined to be distinct for bacteria in each anatomic site. Figure 2 is a Venn diagram illustrating the differences and similarities between the expression profiles of the pneumococci in blood, in CSF, and during ECC. Highlighting the disparity between these conditions, only eight genes had similar alterations in gene expression during bacterial growth in blood, in CSF, or during ECC: two that encode the virulence determinants PspA (46) and PrtA (4), three that encode genes in the *psa* operon (manganese acquisition and transport) (30), two that are involved in energy metabolism (an enolase [*eno*] and a glycosyl hydrolase [SP0265]), and a transporter (SP1587). Their common expression warrants further investigation as potential targets for intervention, since they may reflect a core set of genes required for virulence.

Analysis of gene transcription indicated several features of bacterial physiology unique to each body compartment. Analysis of blood-dependent transcription revealed that cell wall and membrane synthesis, cell division, and competence were unchanged from in vitro. Nonetheless, the pneumococcus appears to be under stress. Supporting this view, 24 genes encoding ribosomal proteins had reduced transcription in the blood. We interpret this as indicating that the pneumococcus is reducing its translational capacity. Likewise, *relA*, the gene encoding the GTP pyrophosphokinase was enhanced during growth in blood (26). RelA is expressed in response to lack of nutrients and is responsible for ppGpp synthesis and entry of the bacteria into the stringent response. Finally, the genes encoding manganese and zinc transporters and the genes responsible for purine and folic acid biosynthesis were also increased.

In the CSF, the pneumococcus decreased transcription of at least 20 genes involved with competence (15), including *comX1*, *comA*, *comB*, *comE*, and *comD*. Likewise, 11 genes involved in the biosynthesis of fatty acids were also markedly reduced. Decreased expression of the *fab* operon (31) may indicate that sufficient fatty acids are available in the CSF. Other differences observed in CSF cultures included enhanced expression of the *lic* operon (50), which indicates that the bacteria are decorating their cell wall with phosphorylcholine. SP1804, a gene encoding a general stress protein, is enhanced in the CSF, perhaps indicating that the bacteria are under stress in adapting from the rich medium of blood to the poor medium of CSF.

Pneumococci adherent to epithelial cells also had unique alterations in their expression profiles. We observed enhanced expression of the *lic* operon (50) and the *dlt* operon (49) during ECC. These changes indicate enhanced addition of phosphorylcholine and D-alanine to teichoic acids. Enhanced expression of VncS and CiaR/H, genes encoding two-component systems (42), indicate global changes in the synthesis of cell wall polymers, peptide pheromones, bacteriocins, and *htrA* expression. Manganese acquisition also appears to be particularly important since the *psa* operon showed enhanced expression in all three of the conditions tested and has recently been shown to undergo enhanced transcription in vivo (30).

With regard to energy metabolism, during growth in blood the pneumococcus reduces the expression of the genes encoding 1-phosphofructokinase and fructose-bisphosphate aldolase. Phosphorylation of 1-phosphofructose by 1-phophofructokinase is the rate-limiting step of glycolysis and targets the molecule for glycolysis (22). Reducing expression levels of 1-phosphofructokinase suggests that the pneumococcus has a readily available carbon source in the blood. At the same time, concurrent enhanced expression of SP0265 and SP2021, glyco-

TABLE 1. Differential expression of *S. pneumoniae* genes as determined by microarray analysis

Gene name and/or description	TIGR annotation[b]	Fold increase or decrease and *P* value[a] in:					
		Blood		CSF		ECC	
		Fold change	*P*	Fold change	*P*	Fold change	*P*
Virulence determinants							
blpU; bacteriocin	SP0041			−3.1	3E-07		
cps4A; capsular polysaccharide biosynthesis	SP0346					2.2	2E-03
cps4C; capsular polysaccharide biosynthesis	SP0348			3.9	2E-12		
pspA; pneumococcal surface protein A	SP0117[A]	3.4	2E-04	50.3	1E-08	4.0	1E-04
cbpJ; choline-binding protein J	SP0378					3.6	9E-07
cbpG; choline-binding protein G	SP0390	1.7	5E-03				
cbpF; choline-binding protein F	SP0391	2.3	2E-03				
blpK; bacteriocin associated protein	SP0533			−2.5	3E-06		
blpY; Immunity protein	SP0545	NA	NA	−16.8	8E-13	NA	NA
prtA; protective antigen A	SP0641[A,D]	15.5	7E-06	9.8	8E-13	3.3	1E-02
spxB; pyruvate oxidase	SP0730			−2.6	6E-06		
lmb; adhesion lipoprotein	SP1002	3.4	2E-05	−5.2	1E-09		
Conserved hypothetical protein	SP1003[A]	8.8	3E-05	−4.6	7E-09		
xseA; exodeoxyribonuclease VII, large subunit	SP1207			−2.2	3E-07		
pln; pneumolysin	SP1923[A]			−5.6	5E-06	−9.8	3E-03
lytA; autolysin	SP1937			−7.6	9E-13		
chpA; choline-binding protein A	SP2190[A]					2.3	2E-02
chpD; choline-binding protein D	SP2201[A]	NA	NA	12.0	2E-12		
htrA; serine protease	SP2239[A]			NA	NA	8.2	4E-05
spoJ; homologous to sporulation protein	SP2240[D]					3.9	9E-05
Cell wall synthesis							
bacA; bacitracin resistance protein	SP0457[B]	2.5	4E-04				
fibA; beta-lactam resistance factor	SP0615					4.0	1E-03
lytB; endo-β-*N*-acetylglucosaminldase	SP0965					3.5	4E-03
licC; phosphocholine cytidytyltransferase	SP1267			4.7	1E-09	14.4	7E-08
licB; choline transport	SP1268			5.1	2E-09	15.4	1E-09
pck; choline kinase	SP1269			4.4	6E-09	18.2	2E-07
Alcohol dehydrogenase, zinc containing	SP1270			5.5	4E-09	17.2	9E-06
Cytidine diphosphocholine pyrophosphorylase, putative	SP1271			5.7	5E-10	14.0	3E-08
pgdA; *N*-acetylglucosamine deacetylase A	SP1479[D]			−3.2	2E-05		
penA; penicillin-binding protein 2B	SP1673					2.4	2E-02
dltD; D-alanyl-lipotechoic acid biosynthesis	SP2173	2.8	7E-04			6.6	1E-03
dltA; D-alanine activating protein	SP2176[A]					3.6	1E-03
Cell membrane							
Lipoprotein	SP0149			3.7	2E-09		
Glycosyl transferase, group 1	SP1366					2.8	6E-04
pgm; phosphoglucomutase	SP1498					−2.1	8E-03
Competence/DNA transformation							
comX1; transcriptional regulator	SP0014			−12.1	6E-11		
Hypothetical protein	SP0029	NA	NA	−8.1	5E-09	NA	NA
ccs16; competence-induced protein Ccs16	SP0030	NA	NA	−16.8	4E-08	NA	NA
comA; competence factor transport protein	SP0042[D]			−32.9	8E-12		
comB; competence factor transport protein	SP0043[D,B]			−48.8	2E-12		
ccs 4; competence-induced protein	SP0200			−5.7	2E-07	3.0	2E-02
Hypothetical protein	SP0201			−2.9	2E-05		
dprA; DNA processing protein	SP1266			−49.7	2E-11	6.2	9E-04
cspC-related protein	SP1913	5.2	8E-04				
cbf1; cmp-binding-factor 1	SP1980			−4.7	2E-09		
ccs50; competence-induced protein	SP1981			−4.5	2E-06		
recA; DNA replication, recombination, and repair	SP1940			−12.9	1E-12		
cinA; competence/damage-inducible protein	SP1941[A]			−39.0	1E-11	2.1	8E-03
Conserved hypothetical protein	SP1944			−2.4	2E-05		
Hypothetical protein	SP1945			−12.1	5E-06		
comE; response regulator ComE	SP2235			−15.0	2E-14	NA	NA
comD; sensor histidine kinase	SP2236[A]			−6.7	2E-08		
Stress related							
hcrA; heat-inducible transcription repressor	SP0515			−4.5	1E-07	−4.4	8E-04

Continued on following page

TABLE 1—*Continued*

Gene name and/or description	TIGR annotation[b]	Fold increase or decrease and *P* value[a] in;					
		Blood		CSF		ECC	
		Fold change	*P*	Fold change	*P*	Fold change	*P*
grpE; heat shock protein	SP0516			−3.7	2E-08	−3.7	2E-03
dnaK; protein folding and stabilization	SP0517			−3.1	6E-06	−3.9	2E-03
sodA; superoxide dismutase	SP0766[A]			−3.5	3E-09		
Cadmium resistance transporter, putative	SP1625			−3.9	1E-10		
Conserved hypothetical protein	SP1644	2.3	3E-04				
relA; GTP pyrophosphokinase	SP1645[A]	2.2	1E-03			2.8	1E-03
Conserved hypothetical protein	SP1801			NA	NA	3.2	4E-03
Hypothetical protein	SP1802					5.5	1E-03
Conserved hypothetical protein	SP1803			NA	NA	4.1	6E-05
General stress protein 24, putative	SP1804			2.7	1E-07	6.7	2E-03
Hypothetical protein	SP1805			3.5	8E-10	3.4	2E-03
groEL; chaperonin, 60 kDa	SP1906			−6.1	4E-11		
groES; chaperonin, 10 kDa	SP1907			−6.9	2E-08		
DNA repair, recombination, and modification							
Conserved hypothetical protein	SP0022	NA	NA	−3.5	4E-06	NA	NA
radA; DNA repair protein	SP0023[AA,C]	NA	NA	−6.3	2E-07	NA	NA
Hypothetical protein	SP0025[D]			−2.8	8E-07		
hexB; DNA mismatch repair protein	SP0173			14.0	5E-14		
Hypothetical protein	SP0792			2.3	4E-08		
MutT/nudix family protein	SP0794			2.0	1E-09		
radC; DNA repair protein	SP1088			−63.2	9E-11		
Type II restriction endonuclease, putative	SP1221					3.0	6E-03
recR; recombination protein	SP1672					2.1	3E-03
recG; ATP-dependent DNA helicase	SP1697					2.6	6E-04
Cell division							
ftsW; cell division protein	SP1067					3.8	5E-03
ppc; phosphoenolpyruvate carboxylase	SP1068[B]					5.0	6E-04
DivlVA; cell division protein	SP1661					1.9	3E-03
y/mH	SP1662					2.2	2E-02
y/mF	SP1664					1.8	4E-02
y/mE	SP1665					2.0	3E-02
spollLJ family protein	SP1975			−2.2	1E-05		
Energy metabolism							
Glycosyl hydrolase, family 1	SP0265[A]	3.5	1E-03	2.2	1E-06	5.5	5E-03
Glycosamine–fructose-6-phosphate	SP0266			2.9	1E-11		
manN; PTS system, IIC component	SP0283					−2.2	7E-03
Alcohol dehydrogenase, zinc-containing	SP0285					−1.7	6E-03
pfl; formate acetyltransferase	SP0459					2.6	7E-04
fba; fructose-bisphosphate aldolase	SP0605			−2.1	1E-07	−2.2	2E-04
Thioredoxin family protein	SP0659[B]	NA	NA	NA	NA	−3.7	2E-04
manA; mannose-6-phosphate isomerase	SP0736			2.7	1E-11	4.2	8E-04
lacR; lactose system repressor	SP0875	−4.8	9E-04				
1-phosphofructokinase, putative	SP0876	−4.0	3E-04				
aid; alanine dehydrogenase, authentic frameshift	SP0952			NA	NA	3.7	2E-03
Phosphoglycerate mutase family protein	SP0984			NA	NA	2.1	4E-03
glgC; glucose-1-phosphate edenylyltransferase	SP1122			3.5	3E-08		
eno; enolase	SP1128	−4.2	3E-03	−2.1	1E-05	−3.3	4E-05
Acetoin dehydrogenase, E1 component	SP1164					2.3	8E-03
lacG; 6-phospho-β-galaciosidase	SP1184			NA	NA	6.5	4E-03
lacB; galactose-6-phosphate isomerase	SP1192			NA	NA	5.9	2E-06
lacA; galactose-6-phosphate isomerase	SP1193[A]			NA	NA	4.2	6E-03
ldh; L-lactate dehydrogenase	SP1220					−2.3	3E-04
fhs; formate-tetrahydrofolate ligase	SP1229					3.9	3E-04
nagB; glucosamine-6-phosphate isomerase	SP1415			−7.5	3E-12		
alpC; ATP synthase F1, epsilon subunit	SP1507					4.8	3E-06
atpD; ATP synthase F1, beta subunit	SP1508					4.0	6E-06
alpG; ATP synthase F1, gamma subunit	SP1509					3.4	5E-04
atpA; ATP synthase F1, alpha subunit	SP1510					4.1	1E-08
atpH; ATP synthase F1, delta subunit	SP1511					3.8	7E-03
atpF; ATP synthase F0, B subunit	SP1512	NA	NA	NA	NA	2.7	4E-04
atpB; ATP synthase F0, A subunit	SP1513					5.3	4E-06

Continued on following page

TABLE 1—*Continued*

Gene name and/or description	TIGR annotation[b]	Fold increase or decrease and *P* value[a] in:					
		Blood		CSF		ECC	
		Fold change	*P*	Fold change	*P*	Fold change	*P*
Glutathione *S*-transferase family protein	SP1550			5.1	2E-05		
Cation-transporting ATPase, E1–E2 family	SP1551			3.7	9E-09		
tpi; triosephosphate isomerase	SP1574					2.2	7E-03
Oxalate formate antiporter	SP1587	3.5	5E-05	4.3	2E-11	3.9	7E-04
gpmA; phosphoglycerate mutase	SP1655	−5.6	3E-03				
ROK family protein	SP1675			6.0	2E-09		
scrR; sucrose operon repressor	SP1725	3.8	4E-03	5.3	9E-10		
galK; galactokinase	SP1853					2.7	3E-03
gap; glyceraldehyde-3-phosphate dehydrogenase	SP2012					−6.5	5E-04
Glycosyl hydrolase, family 1	SP2021			5.8	6E-06	14.5	3E-03
malA; maltose metabolism	SP2111	2.0	8E-04	NA	NA	NA	NA
malR; maltose operon transcriptional repressor	SP2112	3.1	2E-04				
Transketolase, N-terminal subunit	SP2128[A]			NA	NA	5.2	3E-05
PTS system, IIC component, putative	SP2129			NA	NA	6.8	4E-06
argF; ornithine carbamoyltransferase	SP2150					7.6	8E-04
arcC; carbamate kinase	SP2151					9.2	2E-03
Fatty acid metabolism							
cls; cardiolipin synthetase	SP0199[A]					3.6	3E-02
enoyl-CoA[c] hydratase/isomerase family protein	SP0415			−17.3	9E-09	−3.0	6E-04
acp; acyl carrier protein	SP0417	−7.1	7E-04				
fabH; 3-oxoacyl-(acyl carrier protein) synthase III	SP0418			−4.9	3E-07		
fabK; enoyl-(acyl carrier protein) reductase	SP0419			−12.8	2E-09		
fabD	SP0420			−9.8	6E-07		
fabG; 3-oxoacyl- (acyl carrier protein) reductase	SP0421			−13.0	8E-10	−2.1	4E-03
fabF; 3-oxoacyl-(acyl carrier protein) synthase II	SP0422			−10.6	4E-09		
accB; acetyl-CoA carboxylase	SP0423			−10.3	9E-11	−2.1	1E-03
fabZ	SP0424			−6.3	9E-09	−2.1	2E-03
accC; acetyl-CoA carboxylase	SP0425			−10.7	4E-11	−2.3	6E-03
accD; acetyl-CoA carboxylase, subunit beta	SP0426			−8.8	5E-11		
accA; acetyl-CoA carboxylase, subunit alpha	SP0427			−7.7	1E-10		
Amino acid biosynthesis and acquisition							
Amino acid ABC transporter, ATP-binding protein	SP0111			2.3	1E-09		
aliA; oligopeptide ABC transporter	SP0366					3.9	2E-03
ilvB; acetolactate synthase, large subunit	SP0445[A]					7.4	4E-03
ilvN; acetolactate synthase, small subunit	SP0446			2.0	1E-10		
ilvC; ketol-acid reductoisomerase	SP0447					5.5	4E-04
ilvA; threonine dehydratase	SP0450					4.5	5E-04
Transcriptional regulator, MerR family	SP0501			−5.7	1E-10		
Glutamine synthetase, type I	SP0502			−4.4	1E-09		
livH; branched-chain amino acid ABC transporter	SP0750			2.5	2E-06		
livM; branched-chain amino acid ABC transporter	SP0751			2.3	3E-07		
livG; branched-chain amino acid ABC transporter	SP0752			2.3	5E-09		
livF; branched-chain amino acid ABC transporter	SP0753			2.3	3E-07		
Conserved hypothetical protein	SP0783			−4.7	1E-11		
Glutathione reductase	SP0784			−2.2	2E-06		
lcEL; branched-chain amino acid aminotransferase	SP0856[A]					3.5	3E-03
Oligopeptide-binding protein, internal deletion	SP0857					3.8	2E-04
proA; gamma-glutamyl phosphate reductase	SP0932[B]					4.0	3E-03
dapA; dihydrodipicolinate synthase	SP1014			2.6	2E-10	3.6	4E-04

Continued on following page

TABLE 1—*Continued*

Gene name and/or description	TIGR annotation[b]	Fold increase or decrease and *P* value[a] in:					
		Blood		CSF		ECC	
		Fold change	*P*	Fold change	*P*	Fold change	*P*
hemK; conserved protein	SP1021[D]					14.3	1E-04
amiE; ATP-binding protein	SP1888	2.4	6E-05	2.9	1E-08		
amiD; permease protein	SP1889[A]	2.1	1E-04	2.8	9E-09		
AmiC; permease protein	SP1890[A]			2.9	2E-11		
Nucleoside/nucleotride metabolism							
purA; adenylosuccinate synthetase	SP0019			−3.9	5E-09		
Phosphoribosytformylglycinamidine synthase	SP0045[A,C,B]	6.1	5E-05	NA	NA		
purF; amidophosphoribosyltransferase	SP0046	11.6	1E-06	NA	NA		
purM; purine ribonucleotide biosynthesis	SP0047[B]	8.4	1E-05	NA	NA		
purN; purine ribonucleotide biosynthesis	SP0048[B]	9.7	1E-05	NA	NA		
purH; purine ribonucleotide biosynthesis	SP0050[AA]	10.3	4E-06	NA	NA		
purE; purine ribonucleotide biosynthesis	SP0053[C]	3.0	1E-04	NA	NA		
purK; purine ribonucleotide biosynthesis	SP0054[C]	6.9	4E-05				
Hypothetical protein	SP0055	2.4	4E-04	NA	NA		
purB; adenylosuccinate lyase	SP0056[B]	2.7	5E-05				
nrdD; anaerobic ribonucleoside triphosphate	SP0202	2.7	5E-05				
Acetyltransferase. GNAT family	SP0204	3.2	2E-04				
nrdG; anaerobic ribonucleoside-triphosphate	SP0205	3.5	3E-05	5.6	4E-07		
Hypothetical protein	SP0206	2.3	2E-04				
Conserved domain protein	SP0207	2.9	5E-05				
adk; adenylate kinase	SP0231	−3.8	2E-03				
Amino acid biosynthesis and acquisition							
pyrF; orotidine 5-phosphate decarboxylase	SP0701[D]	−6.7	8E-04				
pyrE; orotate phosphoribosyltransferase	SP0702[D]	−11.0	9E-05	NA	NA		
upp; uracil phosphoribosyltransferase	SP0745	−3.9	4E-03				
Hypothetical protein	SP0830					−2.5	3E-03
deoD; purine nucleoside phosphorylase, family 2	SP0831					−3.3	2E-03
pyrK; dihydroorotate dehydrogenase, electron	SP0963	−8.9	7E-05			3.4	IE-03
pyrDb; dihydroorotate dehydrogenase B	SP0964[D]	−5.7	2E-03			4.7	3E-04
carA; carbamoyl-phosphate synthase, small subunit	SP1276	−4.9	9E-04	2.2	2E-06		
pyrB; aspartate carbamoyltransferase	SP1277	−6.9	1E-03	2.0	3E-06		
pyrR; pyrimidine operon regulatory protein	SP1278[AA]	−8.0	8E-05				
uraA; uracil permease	SP1286[A]	−7.7	1E-04				
Oxidoreductase, pyridine nucleotide-disulfide	SP1588	−4.5	8E-04				
Co factor metabolism							
ribAB; riboflavin, FMN, and FAD biosynthesis	SP0176[D,B]	−4.2	8E-04				
ribD; riboflavin, FMN, and FAD biosynthesis	SP0178[D]	−5.4	4E-04				
folC; dihydrofolate synthetase	SP0290	2.1	8E-05			3.1	4E-03
folE; GTP cyclohydrolase I	SP0291	2.3	8E-05				
folE; GTP cyclohydrolase I	SP0291	2.3	8E-05				
Bifunctional lolate synthesis protein	SP0292	2.6	1E-04			2.9	2E-03
coaA; pantothenale kinase	SP0839					5.1	4E-03
Macrolide-efflux protein	SP1110			−4.9	3E-07		
Pyridoxine biosynthesis protein	SP1468			2.8	2E-10		
coaD; phosphopantetheine adenylyltransferase	SP1968			2.3	2E-06		
nadC; pyridine biosynthesis	SP2016			−7.2	1E-07		
Membrane protein	SP2017[A,D]	NA	NA	−15.7	5E-12		
5-Formyltetrahydrofolate cyclo-ligase	SP2095[A]			2.5	4E-10		
Anion/cation aquisition							
Iron							
Non-heme Iron-containing ferritin	SP1572	−8.4	8E-05	−2.4	4E-06		
Alcohol dehydrogenase, iron-containing	SP2026	−3.6	2E-03	NA	NA		
Potassium							
Potassium uptake protein, Trk family	SP0480					2.6	4E-04
Phosphate							
pstA; putative membrane protein	SP1393					2.8	2E-03
Magnesium							
Magnesium transporter, CorA family	SP0185					−2.1	5E-03
Manganese							
psaB; ATP-binding protein	SP1648	7.3	1E-05	5.0	2E-09	3.7	3E-05

Continued on following page

TABLE 1—*Continued*

Gene name and/or description	TIGR annotation[b]	Fold increase or decrease and *P* value[a] in:					
		Blood		CSF		ECC	
		Fold change	*P*	Fold change	*P*	Fold change	*P*
psaC; permease, authentic frameshift	SP1649	9.3	2E-06	4.8	2E-11	7.6	3E-04
psaA; manganese-binding adhesion liprotein	SP1650	9.6	3E-07	5.6	1E-08	8.0	3E-04
Zinc							
adcA; zinc-binding adhesion liprotein	SP2169	9.1	3E-06	NA	NA	NA	NA
adcB; permease protein	SP2170[A]	7.7	1E-05				
adcC; ATP-binding protein	SP2171	6.8	3E-05				
adcR; repressor	SP2172	4.2	8E-06				
Transcription							
mutR; transcriptional regulator	SP0141[AA]	3.0	2E-04				
Conserved hypothetical protein	SP0385[A,D]			−5.0	6E-10		
Sensor histidine kinase, putative	SP0386[D]			−3.9	2E-07		
DNA-binding response regulator	SP0387[D]			−4.3	1E-09		
Hypothetical protein	SP0389			−3.3	2E-06		
Transcriptional regulator, MarR family	SP0416			−5.3	1E-10		
vncS; sensor histidine kinase	SP0604	2.2	5E-04			2.5	1E-02
ciaR; DNA-binding response regulator	SP0798[D]					3.1	4E-03
ciaH; sensor histidine kinase ClaH	SP0799[D]					3.1	1E-03
Transcriptional regulator, putative	SP0908	2.1	7E-04				
Conserved hypothetical protein	SP0909	2.2	2E-03	NA	NA		
prsA; ribose-phosphate pyrophosphokinase	SP1095[D]			−2.5	1E-06		
dnaG; DNA primase	SP1072			−5.2	3E-09		
rpoD; RNA polymerase sigma-70 factor	SP1073			−5.0	4E-06		
Conserved hypothetical protein	SP1074			−4.4	3E-10		
vicX protein	SP1225	2.5	3E-05				
Sensory box sensor histidine kinase	SP1226	2.4	3E-04				
ATP-dependent RNA helicase, putative	SP1586					3.1	1E-05
Transcriptional regulator, Gn1R family	SP1714			−6.6	2E-11		
ABC transporter, ATP-binding protein	SP1715[A,B]			−6.7	1E-08		
Conserved hypothetical protein	SP1716			−12.0	3E-09		
ABC transporter, ATP-binding protein	SP1717[A]			−13.3	1E-10		
marR; transcriptional regulator	SP1863			−2.3	7E-06		
ccpA; catabolite control protein A	SP1999					4.2	3E-03
Translation							
Ribosomal protein S10	SP0208	−4.8	3E-04				
Ribosomal protein L3	SP0209	−4.2	1E-03			2.9	8E-04
Ribosomal protein L23	SP0211	−4.0	4E-03			2.8	2E-05
Ribosomal protein L2	SP0212	−4.1	1E-03				
Ribosomal protein S19	SP0213	−3.9	3E-03				
Ribosomal protein L14	SP0219	−3.6	4E-03				
Translation initiation factor IF	SP0232	−5.0	9E-04				
Ribosomal protein L36	SP0233	−4.5	4E-03				
Ribosomal protein S13	SP0234	−4.7	5E-04				
Ribosomal protein S11	SP0235	−4.4	2E-03				
Ribosomal protein L17	SP0237	−6.1	5E-04				
serS; seryl-tRNA synthetase	SP0411					4.5	6E-03
Ribosomal protein L11	SP0630	−4.7	1E-03				
Ribosomal protein L1	SP0631	−5.0	5E-04				
Ribosomal protein S16	SP0775	−5.2	2E-04				
rpsA; ribosomal protein S1	SP0862					3.7	2E-04
Translation initiation factor IF-3	SP0959	−6.4	6E-05				
Ribosomal protein L35	SP0960	−5.3	3E-03				
Ribosomal protein L20	SP0961	−6.0	9E-04				
Conserved hypothetical protein	SP1097			−3.5	4E-05		
Conserved hypothetical protein	SP1098					2.5	3E-02
Ribosomal large subunit pseudouridine synthase	SP1099			−3.4	5E-05	2.1	2E-02
Ribosomal protein L7/L12	SP1354	−7.8	8E-06				
Ribosomal protein L10	SP1355	−7.3	3E-05				
Ribosomal protein S21	SP1414	−3.8	4E-03				
glyQ; glyl-tRNA synthetase, alpha subunit	SP1475			−3.0	4E-06		
Ribosomal protein S18	SP1539	−4.2	9E-04				
Single-strand binding protein	SP1540	−4.6	9E-04				
Ribosomal protein S6	SP1541	−4.2	5E-03				

Continued on following page

TABLE 1—*Continued*

Gene name and/or description	TIGR annotation[b]	Fold increase or decrease and *P* value[a] in:					
		Blood		CSF		ECC	
		Fold change	*P*	Fold change	*P*	Fold change	*P*
Ribosomal protein S15	SP1626	−3.5	5E-03				
fmt; methionyl-tRNA formyltransferase	SP1735			2.4	1E-07		
oligoendopeptidase F. putative	SP1780[A]	2.9	5E-05				
Conserved hypothetical protein	SP1781	3.2	1E-04				
prmA: ribosomal protein L11 methyltransferase	SP1782[C]	2.4	1E-04				
tgt: queuine tRNA-ribosyltransferase	SP2058			−3.1	1E-05		
Ribosomal subunit interface protein	SP2206			−3.9	2E-07		
Post translational protein alternations							
ABC transporter, ATP-binding protein	SP0151			2.1	1E-06		
ATP-dependent Clp protease	SP0338[A]	NA	NA	−5.8	2E-08	NA	NA
Lipoate-protein ligase, putative	SP1160	3.1	9E-05	2.6	4E-07		
Peptidase, U32 family	SP1429	−5.6	2E-03				
secA: preprotein translocase	SP1702					2.2	4E-03
Serine/threonine protein kinase	SP1732	2.0	2E-03				
Peptidase, M20/M25/M40 family	SP2096					2.9	3E-03
Conserved hypothetical protein	SP2143[A]	NA	NA	NA	NA	11.9	8E-07
Unknown function							
Transporters							
ABC transporter, ATP-binding protein	SP0636			−4.9	1E-07		
Conserved hypothetical protein	SP0638			−4.8	1E-08		
Hypothetical protein	SP0639			−4.0	2E-06		
ABC transporter, ATP-binding protein	SP0786	2.1	1E-04				
Conserved hypothetical protein	SP0787	2.7	2E-04				
ABC transporter, ATP-binding protein	SP1114			NA	NA	−2.9	4E-04
Atz/Trz family protein	SP1356[D]					8.1	9E-06
ABC transporter, ATP-binding/permease protein	SP1357[D]					3.9	4E-03
ABC transporter, ATP-binding/permease protein	SP1358[D]					3.9	2E-04
Glycerol uptake facilitator protein, putative	SP1491					3.4	4E-04
Sodium/dicarboxylate symporter family protein	SP1753					10.2	2E-04
MATE efflux family protein	SP2065			NA	NA	2.4	5E-03
ABC transporter, ATP-binding/permease protein	SP2073	2.2	2E-03	NA	NA	NA	NA
ABC transporter, ATP-binding/permease protein	SP2075[D]					3.0	5E-03
Cation-Transporting ATPase, E1–E2 family	SP2101[A]			2.2	1E-07		
ABC transporter, ATP-binding protein	SP2196			2.3	1E-08		
ABC transporter, substrate-binding protein	SP2197	−4.0	1E-03	−2.8	4E-05		
Unknown							
Hypothetical protein	SP0088			2.9	1E-07		
LysM domain protein	SP0107	2.7	1E-04				
Hypothetical protein	SP0115	18.0	9E-06	NA	NA		
Conserved hypothetical protein	SP0122			−7.8	1E-06		
Hypothetical protein	SP0124			−7.9	1E-06		
Hypothetical protein	SP0125			−3.1	1E-05		
Hypothetical protein	SP0142[D]	13.2	6E-06				
Conserved domain protein	SP0143[D,C]	18.8	2E-05				
Hypothetical protein	SP0144[D]	13.6	1E-05				
Conserved hypothetical protein	SP0145[A,D]	13.0	7E-05				
Conserved hypothetical protein	SP0159	4.4	2E-04				
Hypothetical protein	SP0198[A]					2.1	1E-03
Conserved hypothetical protein	SP0239					3.1	3E-03
Conserved hypothetical protein	SP0288	2.1	8E-04			6.7	3E-04
IS*66* family element: Orf3, degenerate	SP0362					−2.6	4E-03
IS*3*-Spn 1: transposase, degenerate	SP0392					−4.8	8E-04
Conserved hypothetical protein	SP0481			2.3	7E-07		
ABC transporter, ATP-binding protein	SP0483[B]			2.2	5E-12		
Conserved hypothetical protein	SP0488	−4.7	1E-03	−2.9	3E-07		
Hypothetical protein	SP0582			−161.9	3E-15		
Conserved domain protein	SP0617					3.5	1E-03

Continued on following page

TABLE 1—*Continued*

Gene name and/or description	TIGR annotation[b]	Fold increase or decrease and *P* value[a] in:					
		Blood		CSF		ECC	
		Fold change	*P*	Fold change	*P*	Fold change	*P*
Conserved hypothetical protein	SP0629[B]			2.4	6E-07		
Hypothetical protein	SP0703	−4.0	2E-03	NA	NA		
Conserved hypothetical protein	SP0742[C]			−4.3	1E-09		
KH domain protein	SP0776	−5.0	7E-04				
Conserved hypothetical protein	SP0787					3.7	6E-03
Hypothetical protein	SP0800	4.5	2E-05	2.1	4E-06		
Hypothetical protein	SP0816					−3.5	2E-03
Hypothetical protein	SP0833					−2.6	6E-04
Hemolysin-related protein	SP0834					−3.7	3E-03
Conserved hypothetical protein	SP0841			3.3	1E-08		
Conserved hypothetical protein	SP0868			−3.9	5E-07		
NifU family protein	SP0870			−3.5	7E-09		
Conserved hypothetical protein	SP0871					3.2	6E-03
Conserved hypothetical protein	SP0921					−2.2	1E-03
Hypothetical protein	SP0958			−6.7	1E-11		
O-methyltransferase	SP0980[D]			−3.3	6E-06		
Conserved hypothetical protein	SP1012	−7.9	6E-04	NA			
Conserved hypothetical protein	SP1090			−3.9	7E-09		
Conserved domain protein	SP1174[A]	6.6	1E-08	−7.8	2E-14		
Conserved domain protein	SP1175[A]	16.3	1E-07			3.4	1E-02
Conserved hypothetical protein	SP1240	2.7	6E-04				
Conserved hypothetical protein, strain TIGR4	SP1249			3.6	1E-07	6.9	4E-03
lemA	SP1284			−2.1	4E-07		
Transposase family protein, authentic frameshift	SP1484			NA	NA	3.6	6E-04
Methyltransferase, putative	SP1578	3.4	2E-05				
Conserved domain protein	SP1641			−15.5	3E-11		
Hypothetical protein	SP1852[A]	2.1	3E-04	NA	NA		
Nitroreductase family protein	SP1710	NA	NA	2.2	2E-08	NA	NA
Conserved hypothetical protein	SP1716					3.2	8E-03
Hypothetical protein	SP1779[A]	2.8	8E-05				
Hypothetical protein	SP1787			−5.1	8E-09		
Conserved hypothetical protein	SP1875	2.2	9E-05				
Conserved hypothetical protein	SP1876	2.2	1E-04				
Integrase/recombinase, phage integrase family	SP1877	2.1	7E-04				
CBS domain protein	SP1878	2.1	7E-04				
Oxidoreductase, short chain dehydrogenase/reductase	SP1909			5.9	1E-10		
Conserved hypothetical protein	SP1922			−5.8	2E-13		
Hypothetical protein	SP1924			−9.2	2E-09		
Hypothetical protein	SP1925			−4.1	3E-07		
Hypothetical protein	SP1926			−3.7	3E-06		
Conserved hypothetical protein	SP2027[D]			NA	NA	2.6	3E-03
Conserved hypothetical protein	SP2045			−3.0	9E-09		
LysM domain protein, authentic frameshift	SP2063	4.9	5E-06	NA	NA		
Conserved hypothetical protein	SP2132	2.8	1E-03	NA	NA	NA	NA
Conserved hypothetical protein	SP2152					18.2	4E-03
Transporter, truncation	NTL02SP0105	4.2	4E-05				
Hypothetical protein	NTL02SP0107	5.0	6E-05				
Conserved hypothetical protein	NTL02SP0108	13.7	2E-10				
Hypothetical protein	NTL02SP1212	−5.9	2E-04				
Transposon							
IS*66* family element; Orf3, degenerate	SP0362			−11.6	4E-15		
IS*66* family element; Orf3, degenerate	SP0644			−12.9	2E-13		
IS*66* family element; Orf2, Interruption	SP0812			2.5	1E-07		
IS*1381*; transposase OrfA	SP1310			5.3	2E-11		
IS*66* family element; Orf3, degenerate	SP1311			−27.4	3E-07		
IS*1167*; transposase	SP1692			−2.4	3E-06		
IS*1381*; transposase OrfA, internal deletion	SP2137			4.9	4E-08		

[a] Minus (−) fold change values indicate genes with decreased transcription. NA, insufficient data was obtained from the microarray analysis to determine gene expression levels.
[b] Superscript letters: A, identified by STM (13); AA, confirmed by animal infection (13); B, identified by STM (25); C, identified by STM (39); D, identified by DFI (29).
[c] CoA, coenzyme A.

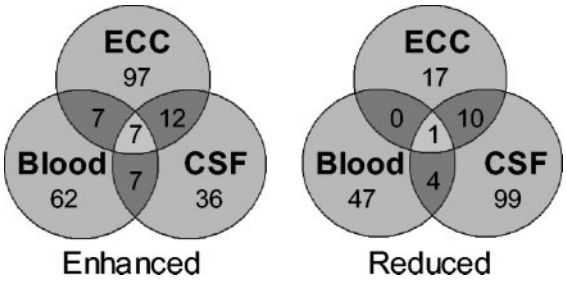

FIG. 2. Venn diagrams highlighting disparity between infectious models for genes with altered expression. Numbers indicate the amount of genes determined to have altered expression that are either shared or exclusive to growth of the pneumococci in blood, CSF, or ECC.

syl hydrolases, and enhanced expression of *scrR* and *malR*, the repressors for sucrose and maltose operons, suggest that the pneumococcus is also utilizing alternative sources of energy.

Phase variation. *S. pneumoniae* undergoes spontaneous phase variation between a transparent phenotype and an opaque phenotype (21); the transparent phenotype has an enhanced capacity to adhere and colonize the nasopharynx, whereas the more phagocytosis-resistant opaque phenotype predominates in blood. An increased capacity to adhere by the transparent phenotype corresponds to higher levels of CbpA, phosphorylcholine, teichoic acid, and autolysin than do opaque variants (21, 41, 48). In contrast, the opaque phenotype produces more capsular polysaccharide and hydrogen peroxide and requires up to 30-fold more human immune serum to achieve 50% opsonophagocytic killing than related transparent strains (20, 43).

Analysis of the genes enhanced during ECC confirmed a selection for the transparent phenotype. We observed enhanced expression of *cbpA* and the *lic* and *dlt* operons. Similar results for bacteria in CSF taken together with downregulation of *spxB* in CSF indicate that the transparent phenotype may reappear after bacteria leave the bloodstream. Interestingly, we did not observe phenotype-enhanced expression of *spxB* or of the genes involved in capsule production in the blood.

Microarray analysis of known virulence determinants. Microarray analysis of 20 known pneumococcal virulence determinants indicated site-specific expression for 17 of them (Table 1). Only two virulence determinants with altered gene expression, *pspA* and *prtA*, were expressed in a similar fashion in blood, CSF, or ECC (see above). *pspA*, encodes a choline-binding protein that inhibits complement deposition on the surface of the bacteria and is upregulated in blood by Northern analysis (46). *prtA* encodes a conserved serine protease (4).

Expression profiles were consistent with much of the current understanding of pneumococcal pathogenesis. During attachment to pharyngeal epithelial cells, pneumococci enhanced expression of the genes encoding choline-binding protein A (CbpA) and HtrA, two proteins shown to contribute to nasopharyngeal colonization (41, 42). Expression of *ply* was decreased, suggesting attenuation of the ability to injure host cells with the toxin pneumolysin. We observed enhanced expression in the blood of the operon encoding choline-binding protein G (CbpG) and choline-binding protein F (CbpF) (12). CbpG has been demonstrated in our laboratory to be required for the development of high-grade bacteremia (preliminary data). Lastly, we observed decreased expression of the genes encoding pneumolysin (*ply*) (8), autolysin (*lytA*) (45), and pyruvate oxidase (*spxB*) (43) in the CSF. Pyruvate oxidase, SpxB, is responsible for the production of hydrogen peroxide by the pneumococcus. This trio was striking since pneumolysin, hydrogen peroxide, and inflammatory cell wall components released by autolysin are the principle agents by which the pneumococcus induces neuronal damage (6, 47). Decreased expression of these genes in the CSF suggests that the pneumococcus adapts so as to decrease damage to neurons.

We also observed alterations in the gene expression of less-well-characterized virulence determinants. In the blood, we observed enhanced expression of *lmb*, a gene homologous to a laminin-binding protein in *Streptococcus anginosus* (1). *lmb* transcription was subsequently reduced in the CSF. Likewise, we observed a decrease in the expression of genes involved in bacteriocin synthesis and immunity (10). These expression profiles suggest a potentially underappreciated role for these genes during pathogenesis.

Cross-reference to STM studies and DFI analyses. Investigators have used STM and DFI to identify pneumococcal genes required for invasive disease (13, 25, 29, 39). In Table 1, we highlight genes with altered expression that have been identified by STM or DFI. Comparison of the three STM studies determined that the majority of loci identified were hit by only one study. Although this may reflect differences in methodology, it is likely that the use of three different strains of *S. pneumoniae*—G54, a serotype 19F (39); strain 0100993, a serotype 3 (25); and T4, a serotype 4 (13)—contributed to the discrepancy observed between the three STM studies. This disparity suggests that strain-dependent variations may occur with regard to virulence. As such, genes identified by more than one method are therefore particularly interesting for the current analysis since they may represent a set of core virulence elements required by all pneumococci for the disease process. Moreover, core genes need not have altered transcription in vivo. The genes encoding immunoglobulin A1 protease (40), ZmpB (a metalloprotease that elicits inflammation in the lower respiratory tract) (5), and PavA (a fibronectin-binding protein) (16) all maintained unchanged levels of expression in vivo and yet were all identified by more than one STM study (Table 2). Table 2 is a comprehensive list of genes with unaltered expression that have been identified by more than one STM study. This approach is not comprehensive, however, since none of the major virulence determinants, such as pneumolysin, capsular polysaccharide, or autolysin, was identified by more than one STM study. This may indicate a more site-specific contribution to pathogenesis (34). Finally, the majority of genes hit by more than one STM analysis encoded proteins whose function is unknown (Table 1). Those whose expression was altered in vivo and that are characterized include the *pur* operon (32) and *rib* operon (23) for purine and riboflavin biosynthesis, respectively, as well as *radA*, a DNA repair enzyme (3).

Virulence assessment of mutants. It is likely that bacterial genes with enhanced expression during invasive disease contribute to the survival of the bacteria in vivo and to the progression of disease. To test this hypothesis, we created mutants in a number of genes of unknown function that were enhanced

TABLE 2. Loci or genes within the same operon identified by multiple STM analyses with constitutive gene expression as determined by in vivo microarray analysis

Gene name	TIGR annotation[a]	Cellular role
iga; immunoglobulin A1 protease	SP0071[A,B]	Pathogenesis: degradation of sIgA
Formate acetyltransferase, putative	SP0251[A,C]	Energy metabolism: fermentation
Transcriptional regulator, putative	SP0306[A,C]	Regulatory functions: other
zmpB; zinc metalloprotease ZmpB	SP664[A,B]	Pathogenesis: protein and peptide secretion degradation of proteins
Transcriptional regulator, LysR family	SP927[A,C]	Regulatory functions: DNA interactions
pavA; adherence and virulence protein A	SP966[A,C]	Pathogenesis: cell adhesion
Cof family protein	SP1291[A]	Unknown
SAP domain protein	SP1292[B]	Unknown
Oxidoreductase, Gfo/Idh/MocA family	SP1482[C]	Unknown substrate
ATP-dependent RNA helicase	SP1483[A]	Transcription
msmK; sugar ABC transporter, ATP-binding protein	SP1580[A,B]	Carbohydrate transport
ROK family protein	SP2142[A,C]	Small molecule interactions
Antigen, cell wall surface anchor protein	SP2145[A,B]	Unknown

[a] Superscript letters: A, identified by STM (13); B, identified by STM (39); C, identified by STM (25).

during ECC or in the bloodstream. Some of these mutants corresponded to genes (SP0090, SP0092, SP1434, and SP2163) that did not meet the criteria listed here. These genes were examined nonetheless due to large changes in gene expression determined in vivo after less-stringent screening (data not shown). Mutants in genes enhanced during ECC were created in T4X and assessed in an intranasal model of infection. Mutants lacking genes enhanced during bacteremia were created in a D39X background and assessed in an intratracheal challenge model of bacteremia. T4X mutants that were determined to be attenuated were then subsequently transferred into a D39X background to identify strain differences (Table 3).

Analysis of mutants made in the T4X background determined that five of seven mutants had a significantly reduced capacity to colonize the nasopharynx. Three of these were completely attenuated and did not cross into the bloodstream, indicating that the genes deleted contributed to the pathogenic potential of the bacteria. Surprisingly, when these three genes were mutagenized in a D39X background, no differences in virulence were observed. This occurred despite the observation that several of the genes mutated in D39X had previously been identified by STM as required for in vivo passage. Bioluminescent imaging of the mice with the Xenogen IVIS camera agreed with bacterial titers collected from lungs of infected

TABLE 3. Virulence assessment of mutants deficient in genes with enhanced expression during ECC or growth in blood

Challenge type and strain	Function	Log_{10} median titer 2 days postchallenger[a] in:				% Survival[c]
		Nasal lavage or lungs[b]		Blood		
		Titer	*P*	Titer	*P*	
Intranasal challenge						
T4X		6.1	NA	5.6	NA	10
T4X SP0090-	ABC transporter, permease	4.3	**0.003**	<3.0	**<0.001**	100
T4X SP0092-	ABC transporter, substrate binding protein	5.7	0.278	4.6	0.107	10
T4X SP0498-	Endo-β-*N*-acetylglucosaminidase, putative	5.5	**0.026**	5.7	0.377	10
T4X SP1021-	*hemK*; conserved protein	5.7	0.088	4.7	0.163	20
T4X SP1753-	Sodium/dicarboxylate symporter family protein	4.5	**0.011**	4.3	0.077	10
T4X SP2143-	Conserved hypothetical protein	5.0	**0.029**	<3.0	**<0.001**	100
T4X SP2163-	PTS system, IIB component	5.1	**0.011**	<3.0	**<0.001**	70
D39X		4.9	NA	7.1	NA	27
D39X SP0090-	ABC transporter, permease protein	4.3	0.119	6.6	0.527	40
D39X SP2143-	Conserved hypothetical protein	4.2	0.111	6.9	0.748	27
D39X SP2163-	PTS system, IIB component	6.2	0.235	7.0	0.852	13
Intratracheal challenge						
D39X		8.4	NA	9.0	NA	0
D39X SP0115-	Hypothetical protein	8.4	0.902	9.1	0.535	0
D39X SP0142-	Hypothetical protein	8.6	0.805	9.1	0.710	0
D39X SP0641-	Serine protease	8.3	1.000	9.0	0.620	0
D39X SP1002-	*lmb*; adhesion lipoprotein	7.2	0.128	9.0	0.620	0
D39X SP1175-	Conserved domain protein	7.5	0.234	8.6	0.181	0
D39X SP1434-	ABC transporter	8.5	0.383	9.2	0.165	0

[a] A total of 12 to 20 mice were used to examine each mutant in both challenge models. Statistical analysis was performed by using a Mann-Whitney rank sum test. Mutant titers were compared to the corresponding wild-type titers. Values in bold face indicate a statistically significant difference. NA, not applicable.
[b] Nasal lavage for intranasal challenge and lungs for intratracheal challenge.
[c] That is, the percent survival 1 week after intranasal challenge or the percent survival 4 days after intratracheal challenge.

mice. These images are thus not shown since they are redundant with the values listed in Table 3. Overall, these results suggest that D39X is can overcome deficiencies in virulence traits that T4X cannot.

Considerations. Although the present study is the first to directly measure pneumococcal gene expression during invasive disease, it must be acknowledged that to obtain sufficient quantities of bacterial RNA from the disease models, certain aspects of the experimental design were not optimal. Foremost, it was necessary to use a different strain for each disease model (D39X for blood, T4X for CSF, and T4R for ECC). Although preliminary data from in vitro experiments (data not shown) demonstrates that D39 and T4 respond in a similar manner to growth in vitro (>99% of the genes examined when grown in C+Y), how each strain responds to different anatomical sites remains unknown. It was also necessary to use a different host species for each disease model (mice for bloodstream infection, rabbits for CSF infection, and humans for ECC), as well as a different RNA extraction protocol for ECC. The relationship between different host species and the pneumococcus may also result in alterations of the pneumococcal response. As a result of these caveats, care must be taken when gene expression levels for different anatomical sites are compared.

A second consideration is the requirement for very high titers of pneumococci in the biological samples and the various durations of infection. For blood, bacterial titers were ca. 10^9 CFU/ml and were collected 2 days after intratracheal challenge. As such, the expression profile observed does not represent the initial phases of bloodstream infection. Likewise, rabbits were infected intracisternally with 10^8 CFU, and the bacteria were collected 4 h later. Since the bacteria were collected after only 4 h, our model represents bacterial gene expression during early meningitis. During a natural infection, only a few animals would have a bacterial titer as high as 10^8 CFU/ml in the CSF, and leukocytes and other host factors would be present in the CSF.

A final consideration is that not all of the genes in the genome were examined. Although our analysis of in vivo gene expression is the most comprehensive to date, we were unable to report on the expression of 31% of the genome during growth in blood, 47% in the CSF, and 32% after ECC. As such, the present study is not comprehensive and further studies, including confirmation by Northern analysis of specific genes, are warranted.

Conclusions. Microarray analysis of pneumococcal gene expression during invasive disease sheds light on the complex mechanisms of pneumococcal pathogenesis. Despite limitations imposed by technical challenges associated with in vivo RNA collection, we observed dramatic changes in a variety of genes, thus providing important information as to the physiology of the pneumococcus during invasive disease. Most genes (~90%) do not change expression from in vitro growth medium to in vivo. However, strikingly, the pneumococcus seems to adapt to the blood, CSF, and ECC in a site-specific manner. These changes may be a result of the pneumococcus adapting to nutrient availability and the stresses placed on the bacteria. In blood, cell wall and membrane synthesis and competence were unchanged, whereas the bacteria strongly decreased ribosomal transcription, reduced glycolysis, and increased CbpG and CbpF. In CSF, pneumococci drastically curtailed gene expression for competence, autolysis, and production of toxins, while increasing amino acid biosynthesis and choline on the cell surface.

Cross-referencing of microarray analyses with that of STM and DFI and the virulence assessment of our own mutants strongly implies that pneumococcal virulence is dependent on a network of genes, the majority of which are not fully understood. Although an understanding of this network may seem daunting, it seems that the continued use of global analytical techniques will shed light on the core genes that are required for virulence. Such an attempt will require synthesis of data from multiple strains to derive a general picture of virulence above the noise of strain variation.

ACKNOWLEDGMENTS

We thank Robert Fleischmann and Scott Peterson at the PFGRC at TIGR for providing the pneumococcal microarrays necessary for this project. We also thank Alessandra Polissi, Sauli Haataja, and Jeremy Brown for providing data from their STM studies.

This study was supported by NIH grant R01 AI27913 and The American Lebanese Syrian Associated Charities.

REFERENCES

1. **Allen, B. L., and M. Hook.** 2002. Isolation of a putative laminin binding protein from *Streptococcus anginosus.* Microb. Pathog. **33:**23–31.
2. **Avery, O. T., C. M. MacLeod, and M. McCarty.** 1944. Studies on the chemical nature of the substance inducing transformation of the pneumococcal types: induction of transformation by the deoxyribonucleic acid fraction isolated from pneumococcus type III. J. Exp. Med. **79:**137–157.
3. **Beam, C. E., C. J. Saveson, and S. T. Lovett.** 2002. Role for *radA/sms* in recombination intermediate processing in *Escherichia coli.* J. Bacteriol. **184:** 6836–6844.
4. **Bethe, G., R. Nau, A. Wellmer, R. Hakenbeck, R. R. Reinert, H. P. Heinz, and G. Zysk.** 2001. The cell wall-associated serine protease PrtA: a highly conserved virulence factor of *Streptococcus pneumoniae.* FEMS Microbiol. Lett. **205:**99–104.
5. **Blue, C. E., G. K. Paterson, A. R. Kerr, M. Berge, J. P. Claverys, and T. J. Mitchell.** 2003. ZmpB, a novel virulence factor of *Streptococcus pneumoniae* that induces tumor necrosis factor alpha production in the respiratory tract. Infect. Immun. **71:**4925–4935.
6. **Braun, J. S., J. E. Sublett, D. Freyer, T. J. Mitchell, J. L. Cleveland, E. I. Tuomanen, and J. R. Weber.** 2002. Pneumococcal pneumolysin and H_2O_2 mediate brain cell apoptosis during meningitis. J. Clin. Investig. **109:**19–27.
7. **Bricker, A. L., and A. Camilli.** 1999. Transformation of a type 4 encapsulated strain of *Streptococcus pneumoniae.* FEMS Microbiol. Lett. **172:**131–135.
8. **Cockeran, R., R. Anderson, and C. Feldman.** 2002. The role of pneumolysin in the pathogenesis of *Streptococcus pneumoniae* infection. Curr. Opin. Infect. Dis. **15:**235–239.
9. **Darkes, M. J., and G. L. Plosker.** 2002. Pneumococcal conjugate vaccine (Prevnar; PNCRM7): a review of its use in the prevention of *Streptococcus pneumoniae* infection. Paediatr. Drugs **4:**609–630.
10. **de Saizieu, A., C. Gardes, N. Flint, C. Wagner, M. Kamber, T. J. Mitchell, W. Keck, K. E. Amrein, and R. Lange.** 2000. Microarray-based identification of a novel *Streptococcus pneumoniae* regulon controlled by an autoinduced peptide. J. Bacteriol. **182:**4696–4703.
11. **Francis, K. P., J. Yu, C. Bellinger-Kawahara, D. Joh, M. J. Hawkinson, G. Xiao, T. F. Purchio, M. G. Caparon, M. Lipsitch, and P. R. Contag.** 2001. Visualizing pneumococcal infections in the lungs of live mice using bioluminescent *Streptococcus pneumoniae* transformed with a novel gram-positive *lux* transposon. Infect. Immun. **69:**3350–3358.
12. **Gosink, K. K., E. R. Mann, C. Guglielmo, E. I. Tuomanen, and H. R. Masure.** 2000. Role of novel choline binding proteins in virulence of *Streptococcus pneumoniae.* Infect. Immun. **68:**5690–5695.
13. **Hava, D. L., and A. Camilli.** 2002. Large-scale identification of serotype 4 *Streptococcus pneumoniae* virulence factors. Mol. Microbiol. **45:**1389–1406.
14. **Hava, D. L., J. LeMieux, and A. Camilli.** 2003. From nose to lung: the regulation behind *Streptococcus pneumoniae* virulence factors. Mol. Microbiol. **50:**1103–1110.
15. **Havarstein, L. S.** 1998. Identification of a competence regulon in *Streptococcus pneumoniae* by genomic analysis. Trends Microbiol. **6:**297–300.
16. **Holmes, A. R., R. McNab, K. W. Millsap, M. Rohde, S. Hammerschmidt, J. L. Mawdsley, and H. F. Jenkinson.** 2001. The *pavA* gene of *Streptococcus pneumoniae* encodes a fibronectin-binding protein that is essential for virulence. Mol. Microbiol. **41:**1395–1408.

17. **Hoskins, J., W. E. Alborn, Jr., J. Arnold, L. C. Blaszczak, S. Burgett, B. S. DeHoff, S. T. Estrem, L. Fritz, D. J. Fu, W. Fuller, C. Geringer, R. Gilmour, J. S. Glass, H. Khoja, A. R. Kraft, R. E. Lagace, D. J. LeBlanc, L. N. Lee, E. J. Lefkowitz, J. Lu, P. Matsushima, S. M. McAhren, M. McHenney, K. McLeaster, C. W. Mundy, T. I. Nicas, F. H. Norris, M. O'Gara, R. B. Peery, G. T. Robertson, P. Rockey, P. M. Sun, M. E. Winkler, Y. Yang, M. Young-Bellido, G. Zhao, C. A. Zook, R. H. Baltz, S. R. Jaskunas, P. R. Rosteck, Jr., P. L. Skatrud, and J. I. Glass.** 2001. Genome of the bacterium *Streptococcus pneumoniae* strain R6. J. Bacteriol. **183:**5709–5717.
18. **Jedrzejas, M. J.** 2001. Pneumococcal virulence factors: structure and function. Microbiol. Mol. Biol. Rev. **65:**187–207.
19. **Kerr, M. K., and G. A. Churchill.** 2001. Bootstrapping cluster analysis: assessing the reliability of conclusions from microarray experiments. Proc. Natl. Acad. Sci. USA **98:**8961–8965.
20. **Kim, J. O., S. Romero-Steiner, U. B. Sorensen, J. Blom, M. Carvalho, S. Barnard, G. Carlone, and J. N. Weiser.** 1999. Relationship between cell surface carbohydrates and intrastrain variation on opsonophagocytosis of *Streptococcus pneumoniae.* Infect. Immun. **67:**2327–2333.
21. **Kim, J. O., and J. N. Weiser.** 1998. Association of intrastrain phase variation in quantity of capsular polysaccharide and teichoic acid with the virulence of *Streptococcus pneumoniae.* J. Infect. Dis. **177:**368–377.
22. **Kornberg, H. L.** 2001. Routes for fructose utilization by *Escherichia coli.* J. Mol. Microbiol. Biotechnol. **3:**355–359.
23. **Kreger, A. S., and R. H. Olsen.** 1968. Purification and properties of mutant and wild-type diaphorases from *Diplococcus pneumoniae.* J. Bacteriol. **96:** 1029–1036.
24. **Lacks, S., and R. D. Hotchkiss.** 1960. A study of the genetic material determining an enzyme activity in the pneumococcus. Biochim. Biophys. Acta **39:**508–517.
25. **Lau, G. W., S. Haataja, M. Lonetto, S. E. Kensit, A. Marra, A. P. Bryant, D. McDevitt, D. A. Morrison, and D. W. Holden.** 2001. A functional genomic analysis of type 3 *Streptococcus pneumoniae* virulence. Mol. Microbiol. **40:** 555–571.
26. **Lemos, J. A., T. A. Brown, Jr., and R. A. Burne.** 2004. Effects of RelA on key virulence properties of planktonic and biofilm populations of *Streptococcus mutans.* Infect. Immun. **72:**1431–1440.
27. **Madu, A., C. Cioffe, U. Mian, M. Burroughs, E. Tuomanen, M. Mayers, E. Schwartz, and M. Miller.** 1994. Pharmacokinetics of fluconazole in cerebrospinal fluid and serum of rabbits: validation of an animal model used to measure drug concentrations in cerebrospinal fluid. Antimicrob. Agents Chemother. **38:**2111–2115.
28. **Mandell, L. A.** 1995. Community-acquired pneumonia: etiology, epidemiology, and treatment. Chest **108:**35S–42S.
29. **Marra, A., J. Asundi, M. Bartilson, S. Lawson, F. Fang, J. Christine, C. Wiesner, D. Brigham, W. P. Schneider, and A. E. Hromockyj.** 2002. Differential fluorescence induction analysis of *Streptococcus pneumoniae* identifies genes involved in pathogenesis. Infect. Immun. **70:**1422–1433.
30. **Marra, A., S. Lawson, J. S. Asundi, D. Brigham, and A. E. Hromockyj.** 2002. In vivo characterization of the *psa* genes from *Streptococcus pneumoniae* in multiple models of infection. Microbiology **148:**1483–1491.
31. **Marrakchi, H., K. H. Choi, and C. O. Rock.** 2002. A new mechanism for anaerobic unsaturated fatty acid formation in *Streptococcus pneumoniae.* J. Biol. Chem. **277:**44809–44816.
32. **Ng, W. L., K. M. Kazmierczak, G. T. Robertson, R. Gilmour, and M. E. Winkler.** 2003. Transcriptional regulation and signature patterns revealed by microarray analyses of *Streptococcus pneumoniae* R6 challenged with sublethal concentrations of translation inhibitors. J. Bacteriol. **185:**359–370.
33. **Ogunniyi, A. D., P. Giammarinaro, and J. C. Paton.** 2002. The genes encoding virulence-associated proteins and the capsule of *Streptococcus pneumoniae* are upregulated and differentially expressed in vivo. Microbiology **148:**2045–2053.
34. **Orihuela, C. J., G. Gao, K. P. Francis, J. Yu, and E. Tuomanen.** Tissue-specific contributions of pneumococcal virulence factors to pathogenesis. J. Infect. Dis., in press.
35. **Orihuela, C. J., G. Gao, M. McGee, J. Yu, K. P. Francis, and E. I. Tuomanen.** 2003. Organ-specific models of *Streptococcus pneumoniae* disease. Scand. J. Infect. Dis. **35:**647–652.
36. **Orihuela, C. J., R. Janssen, C. W. Robb, D. A. Watson, and D. W. Niesel.** 2000. Peritoneal culture alters *Streptococcus pneumoniae* protein profiles and virulence properties. Infect. Immun. **68:**6082–6086.
37. **Pearce, B. J., Y. B. Yin, and H. R. Masure.** 1993. Genetic identification of exported proteins in *Streptococcus pneumoniae.* Mol. Microbiol. **9:**1037–1050.
38. **Peterson, W. D., Jr., C. S. Stulberg, and W. F. Simpson.** 1971. A permanent heteroploid human cell line with type B glucose-6-phosphate dehydrogenase. Proc. Soc. Exp. Biol. Med. **136:**1187–1191.
39. **Polissi, A., A. Pontiggia, G. Feger, M. Altieri, H. Mottl, L. Ferrari, and D. Simon.** 1998. Large-scale identification of virulence genes from *Streptococcus pneumoniae.* Infect. Immun. **66:**5620–5629.
40. **Poulsen, K., J. Reinholdt, and M. Kilian.** 1996. Characterization of the *Streptococcus pneumoniae* immunoglobulin A1 protease gene (*iga*) and its translation product. Infect. Immun. **64:**3957–3966.
41. **Rosenow, C., P. Ryan, J. N. Weiser, S. Johnson, P. Fontan, A. Ortqvist, and H. R. Masure.** 1997. Contribution of novel choline-binding proteins to adherence, colonization, and immunogenicity of *Streptococcus pneumoniae.* Mol. Microbiol. **25:**819–829.
42. **Sebert, M. E., L. M. Palmer, M. Rosenberg, and J. N. Weiser.** 2002. Microarray-based identification of *htrA*, a *Streptococcus pneumoniae* gene that is regulated by the CiaRH two-component system and contributes to nasopharyngeal colonization. Infect. Immun. **70:**4059–4067.
43. **Spellerberg, B., D. R. Cundell, J. Sandros, B. J. Pearce, I. Idanpaan-Heikkila, C. Rosenow, and H. R. Masure.** 1996. Pyruvate oxidase, as a determinant of virulence in *Streptococcus pneumoniae.* Mol. Microbiol. **19:**803–813.
44. **Tettelin, H., K. E. Nelson, I. T. Paulsen, J. A. Eisen, T. D. Read, S. Peterson, J. Heidelberg, R. T. DeBoy, D. H. Haft, R. J. Dodson, A. S. Durkin, M. Gwinn, J. F. Kolonay, W. C. Nelson, J. D. Peterson, L. A. Umayam, O. White, S. L. Salzberg, M. R. Lewis, D. Radune, E. Holtzapple, H. Khouri, A. M. Wolf, T. R. Utterback, C. L. Hansen, L. A. McDonald, T. V. Feldblyum, S. Angiuoli, T. Dickinson, E. K. Hickey, I. E. Holt, B. J. Loftus, F. Yang, H. O. Smith, J. C. Venter, B. A. Dougherty, D. A. Morrison, S. K. Hollingshead, and C. M. Fraser.** 2001. Complete genome sequence of a virulent isolate of *Streptococcus pneumoniae.* Science **293:**498–506.
45. **Tomasz, A., and S. Waks.** 1975. Mechanism of action of penicillin: triggering of the pneumococcal autolytic enzyme by inhibitors of cell wall synthesis. Proc. Natl. Acad. Sci. USA **72:**4162–4166.
46. **Tu, A. H., R. L. Fulgham, M. A. McCrory, D. E. Briles, and A. J. Szalai.** 1999. Pneumococcal surface protein A inhibits complement activation by *Streptococcus pneumoniae.* Infect. Immun. **67:**4720–4724.
47. **Tuomanen, E., B. Hengstler, O. Zak, and A. Tomasz.** 1986. Induction of meningeal inflammation by diverse bacterial cell walls. Eur. J. Clin. Microbiol. **5:**682–684.
48. **Weiser, J. N., R. Austrian, P. K. Sreenivasan, and H. R. Masure.** 1994. Phase variation in pneumococcal opacity: relationship between colonial morphology and nasopharyngeal colonization. Infect. Immun. **62:**2582–2589.
49. **Whiting, G. C., and S. H. Gillespie.** 1996. Investigation of a choline phosphate synthesis pathway in *Streptococcus pneumoniae*: evidence for choline phosphate cytidylyltransferase activity. FEMS Microbiol. Lett. **143:**279–284.
50. **Zhang, J. R., I. Idanpaan-Heikkila, W. Fischer, and E. I. Tuomanen.** 1999. Pneumococcal *licD2* gene is involved in phosphorylcholine metabolism. Mol. Microbiol. **31:**1477–1488.

Editor: J. N. Weiser